Int. J. Electrochem. Sci., 9 **(2014)** 4257 - 4267

International Journal of
ELECTROCHEMICAL
SCIENCE
www.electrochemsci.org

A Study of Transient Phase Transformation in LFS/C using in-situ Time Resolved X-ray Absorption Spectroscopy

Onlamee Kamon-in[1], *Sunisa Buakeaw*[2], *Wantana Klysubun*[3],*Wanwisa Limphirat*[3], *Sutham Srilomsak*[1,4] *and Nonglak Meethong*[5,6,7,*]

[1]School of Ceramic Engineering, Suranaree University of Technology, Nakhon Ratchasima, 30000, Thailand
[2]Materials Science and Nanotechnology Program, Faculty of Science, Khon Kaen University, Khon Kaen, 40002, Thailand
[3]Synchrotron Light Research Institute, Nakhon Ratchasima, 30000, Thailand
[4]Nanotec-SUT Center of Excellence on Advanced Functional Nanomaterials, Suranaree University of Technology, Nakhon Ratchasima, 30000, Thailand
[5]Department of Physics, Faculty of Science, Khon Kaen University, Khon Kaen, 40002, Thailand
[6]Nanotec-KKU Center of Excellence on Advanced Nanomaterials for Energy Production and Storage, Khon Kaen University, Khon Kaen,40002 , Thailand
[7]Intregated Nanotechnology Research Center, Khon Kaen University, Khon Kaen, 40002, Thailand
[*]E-mail: nonmee@kku.ac.th

Received: 24 March 2014 / *Accepted:* 18 April 2014 / *Published:* 19 May 2014

Li_2FeSiO_4 (LFS) is one of the most studied materials for use as cathodes in next generation high capacity Li-ion batteries. In this work, high purity and nanosized LFS/C material with the monoclinic crystal structure in $P2_1$ space group are studied. Structural transformations upon cycling and during relaxation of the high performance LFS/C material are investigated using in situ time resolved X-ray absorption spectroscopy (XAS). Results show that phase transformation involving the present of Fe ion in the Fe4+state when cycling above 4.43 V is responsible for high capacity characteristics in this LFS/C material. The Fe *K*-edge energy variations during relaxation indicate that local structural and oxidation state of Fe also change. This transient change in local structure of Fe in LFS materials is captured by this technique for the first time.

Keywords: local structure transformation; relaxation; in-situ absorption spectroscopy; Li_2FeSiO_4

1. INTRODUCTION

The need for more efficient, safe, low cost, and long lived Li-ion batteries for applications such as electric vehicles (EV) and large-scale storage for solar and wind energy has drawn attention of

researchers around the world to search for new materials for the future batteries [1]. Lithium iron silicate (Li_2FeSiO_4 or LFS) is one of the materials being investigated for a potential use as a cathode in the next generation high capacity Li-ion batteries. LFS has a theoretical specific charge capacity of 166 $mAh.g^{-1}$ by transferring one Li-ion per unit formula from cathode to anode during a charging process [2-3]. However, if enough potential is applied to enable the insertion/extraction of two Li-ions per unit formula, a specific capacity of 332 $mAh.g^{-1}$[4] is achievable. This material can crystallize in various crystal structures and which structure gives the best electrochemical performance is still being investigated. LFS material was first successfully synthesized by a solid-state reaction at 700ºC and had an orthorhombic crystal structure under the $Pmn2_1$ space group [2]. Synthesizing this material at 800ºC using the same method as in [2] resulted in LFS material with a monoclinic crystal structure under $P2_1$ and $P2_1/m$ space groups [5]. LFS preparation by solid-state reactions under an argon atmosphere quenched from 900ºC gave LFS material with an orthorhombic crystal structure under the *Pmnb* space group [6,7]. Generally, specific discharge capacity prepared in the above mentioned work was around 160 $mAh.g^{-1}$ indicating that only one Li-ion per formula unit was utilized. Electrode materials prepared by solid state reactions regardless of their crystal structure generally have poor electrical conductivity due to their large particle size. Carbon coating technique and using nanosize materials are two most common approaches to improve this drawback. Carbon coating in LFS material has been done by adding carbon from different sources such as sucrose or carbon black [8], citric acid [9], glucose or pith [10], carbon nanotubes [11], L-ascorbic acid [12] and starch solution [13]. Reduction of particle size or altering shape can also improve the electrochemical performance of LFS material. For example, Lv et al. [14] reported that by synthesizing 40-50 nm LFS material via a solution-polymerization approach, the initial discharge capacity of approximately 220 $mAh.g^{-1}$ was achieved. Rangappa et al. [15] later reported that an ultrathin nano-sheets of LFS synthesized by a supercritical fluid method exhibited a specific capacity of approximately 340 $mAh.g^{-1}$when cycled at 45ºC. Both of these work show that more than one Li-ions per formula unit can be extracted from the LFS lattice.

In spite of major improvements regarding the electrochemical performance of this material, knowledge of the local structure of LFS in various polymorphs, which is important to understand the mechanisms during the intercalation processes and optimizing the structure of this material is still lacking. Different polymorphs may have different phase transformation mechanisms. At the moment, the relationship between the crystal structure and electrochemical properties, which is crucial to understanding the mechanism of charge/discharge and optimizing the structure of materials, is still unknown. X-ray absorption spectroscopy (XAS) can be used to study local, atomic, and electronic structures, as well as to study the stability of electrode materials [16]. In-situ XAS has been used to monitor the structural changes during Li-extraction/insertion in battery materials through analyzes of X-ray Absorption Near Edge Structure (XANES) and Extended X-ray Absorption Fine Structure (EXAFS) spectra. Although only about one Li-ion per unit formula was investigated, Dominko et al. [17] reported an in-situ XAS study of LFS with space group $Pmn2_1$ to show that the local symmetry of Fe cations could reversibly return to the initial one after cycling. Later, Lv et al. [18] reported an in-situ XAS study of the LFS with space group $Pmn2_1$ during the charging process from open circuit

potential to 4.8 V and showed that Fe ion was oxidized continuously during the charging process indicating that LFS undergone two two-phase reactions when the electrode was charged above 4.1 V.

In the current study, the poly (ethylene oxide)- poly (propylene oxide)-poly (ethylene oxide) triblock copolymer (Pluronic®P-123) was used as a carbon source to synthesize nanosize LFS/C material with $P2_1$ space group. The LFS/C material is very stable and shows high reversible capacities of more than 200 $mAh.g^{-1}$ at a current density of C/3 (1C = 166 $mA.g^{-1}$). Rate capability of this material is also excellent. The local structures of the LFS/C with $P2_1$ space group during charging and discharging processes between 1.5-4.8 V during battery operation and during relaxation are investigated by *in-situ* XAS for the first time.

2. EXPERIMENTAL

2.1 Preparation of LFS/C material

LFS/C material was synthesized by a sol-gel method using lithium acetate dehydrate (98% purity, Acros), iron(III) nitrate nonahydrate (98% purity, Acros), and tetraethyl orthosilicate (TEOS, 98% purity, Acros) as raw materials. The poly (ethylene oxide)- poly (propylene oxide)-poly (ethylene oxide) triblock copolymer (Pluronic®P-123) was used as an effective source of carbon coating as proposed by Xiaozhen et al [19]. During preparation, 1g of Pluronic®P-123 was dissolved in 20 ml of absolute alcohol under magnetic stirring. Afterward, 0.002 mol of tetra ethyl orthosilicate was added to the solution. Then, a stoichiometric amount of lithium acetate dehydrate and iron(III) nitrate nonahydrate were added to the mixture, respectively. After mixing for 2 hours at room temperature, a clear crimson solution was obtained. The crimson solution was transformed into a wet gel after evaporating off the solvent for 5 hours at room temperature. The wet gel was dried in a vacuum oven at 100 ºC for 24 hours. The precursor was ground and calcined in a quartz tube at 650 ºC for 12 hours under an Ar atmosphere (Grade 5, 99.999% purity).The resulting black powder of LFS/C material was kept in a dry glove box for future use.

2.2 Characterizations of the material

The phase purity and crystal structure of the LFS/C material were determined by X-ray diffraction (XRD) using a Bruker D-2 diffractometer with a Cu-K_α radiation. Structural parameters were analyzed by a Rietveld refinement method. The *in-situ* XAS experiments were conducted at Beamline2.2 [20,21] at the Synchrotron Light Research Institute(SLRI) in Thailand. XANES spectra of Fe *K*-edge (7112 eV) were collected at different states of charge and discharge during battery operation over a voltage range of 1.5-4.8 V as well as during relaxation. Transmission detection mode was selected using a Ge(220) double crystal monochromator at BL8 and a Si(111) at BL2.2 over an energy range of 3440-10000 eV. The photon energy was calibrated using an iron foil. All the XANES spectra were averaged and normalized using IFFEFIT software version 1.2.11 [22].

2.3 Electrode preparation and in-situ battery cell

For cathode preparation, the LFS/C material, conductive carbon (superP) and binder (Kynar2801) with a weight ratio of 78:11:11 were thoroughly mixed in a speed mill for 2 hours using N-methyl-2-pyrolidene (NMP) as the solvent. The slurry was casted on aluminum foil, which was used as current collector, with active material loadings of 3-5 mg.cm^{-2}. Finally, the *in-situ* cell was assembled in a dry and inert Ar filled glovebox using the prepared cathode, micro-porous polymer (Celgard2400) as a separator, lithium ribbons as anode and a liquid solution of $LiPF_6$ electrolyte containing ethylene carbonate: dimethyl carbonate: diethyl carbonate (EC:DMC:DEC), in a volume ratio of 1:1:1. The electrochemical performance was measured using galvanostatic cycling method, in which various current densities were applied over the voltage range of 1.5-4.8 V at 30 °C.

3. RESULTS AND DISCUSSION

3.1. Crystal structure and morphology of the LFS/C material

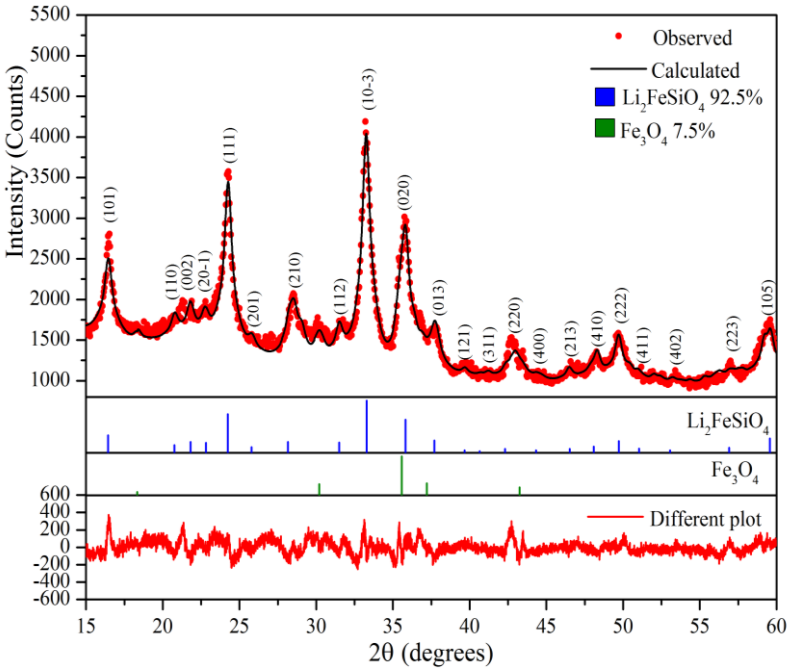

Figure 1. XRD pattern and refinement of the LFS/Cmaterial indexed in the space group $P2_1$ which corresponds to the monoclinic structure with a = 8.2504(1) Å, b = 5.0029(5) Å, c = 8.2131(6) Å, beta angle (β) = 98.56(1), R_{wp} = 4.57%, R_p = 3.66% and R_{exp} = 2.75%.

X-ray diffraction pattern of the LFS/C material in Fig. 1 shows that the LFS/C synthesized at 650°C can be indexed on the basis of a monoclinic unit cell in space group $P2_1$. This is consistent with a similar product reported by Xiaozhen et al. [19]. Nevertheless, at this temperature, a small amount of Fe_3O_4 (magnetite) impurity is also present. The lattice parameters of the LFS/C determined from the Rietveld refinement method using starting parameters from Nishimura et al.[5] are *a = 8.2504(1) Å, b*

= 5.0029(5) Å, c = 8.2131(6) Å, and *beta angle (β) = 98.56(1)*. The XRD peaks are quite broad due to the nano-crystalline nature of the material. The crystallite size of the LFS/C powder was calculated using the Scherrer's equation to be approximately 16 nm. Transmission electron microscopy image as shown in Fig. 2 indicates that the nanoparticles have a round shape with quite narrow particle size distribution. The average particle size is around 15-20 nm, which is consistent with the calculated average crystallite size from XRD.

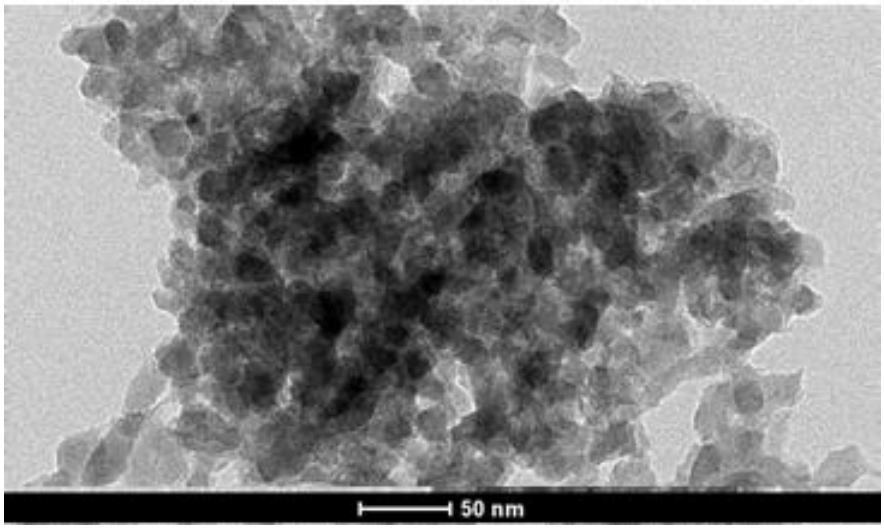

Figure 2. TEM image of the LFS/C powder

3.2. Electrochemical properties of Li_2FeSiO_4/C

Some examples of the charge and discharge profiles measured at various current rates of the LFS/C cathode prepared by the sol-gel method using tri-block copolymer P123 as the carbon source are shown in Fig. 3. The sol-gel method is known to produce small particle size and by reducing the particles size the diffusion path length of the Li ions inactive materials during intercalation is shorten and the ionic conductivity is improved. Adding carbon can also suppress the particle growth and improve electronic conductivity. Fig. 3 reveals that the LFS/C cathode delivered high specific charge and discharge capacities of greater than 280 $mAh.g^{-1}$ and 200 $mAh.g^{-1}$ corresponding to greater than 1.7 and 1.2 Li^+ ion per formula unit at low current densities of C/10 and C/3, respectively. At higher current densities of 1C and 3C, the LFS/C cathode prepared in this work still show high reversible capacities of 150 $mAh.g^{-1}$ and 115 $mAh.g^{-1}$. This results show that using nanosized particles combined with conductive carbon coating are effective to improve electrochemical properties of this material and more than 1 Li^+ ion per formula unit can be reversibly inserted into or removed from its structure. It is noticeable that upon cycling at relatively high current densities, this material shows better stability and reversibility than cycling at low current rates. For example, the discharge capacities measured at the current density of 3C over 10 cycles stay almost unchanged resulting in the curves that lie on top of each other. The discharge capacities measured at C/3-rate fade from 210 $mAh.g^{-1}$ to 200 $mAh.g^{-1}$ over 6 cycles. This result indicates that the LFS/C cathode may be more suitable for use in high power

applications such as in hybrid vehicles than in low rate applications.

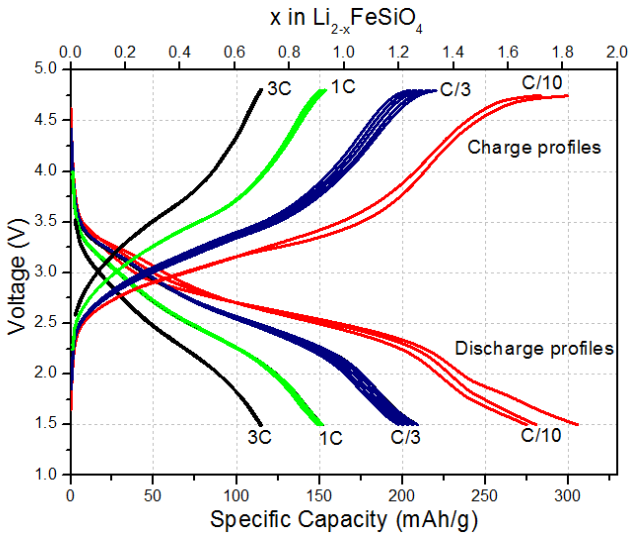

Figure 3. Charge and discharge profiles of the LFS/C cathode measured at various current densities between 1.5-4.8 V (*vs*. Li^+/Li).

Also seen in Fig.3, shape of the charge profiles especially at low current rates apparently shows two distinct regions. The first region at lower voltages shows that the curves have high tangent slopes and should be resulting from phase transformation involving the oxidation of Fe^{2+} to Fe^{3+}. The second region at higher voltages is relatively flatter and should indicate partial oxidation of Fe^{3+} to Fe^{4+}. The discharge curves also show two regions with a less obvious distinction, which should be correlated to reduction of Fe-ion to lower oxidation state upon re-insertion of the Li ions back into the LFS structure. The oxidation and reduction peaks are a clear signature of phase transition similar to previous report for high capacity LFS [23].

3.3. Structure transformation during battery operation

The origin of the observed high capacity in our material is studied by *in-situ* XANES experiments since this technique can be used to directly differentiate XANES spectra of Fe-ion from various oxidation states. Fig. 4 (a) shows the charge-discharge profiles of the LFS/C cathode during the *in-situ* time resolved XAS experiments. The voltages at which the Fe *K*-edge XANES spectra were measured are also indicated on the plot. The open circles indicate the voltages during relaxation (no current applied). The Fe *K*-edge XANES spectra during the relaxation process are collected, and results will be discussed in the next section. The Fe *K*-edge XANES spectra during charge and discharge processes between 1.5-4.8 V are shown in Fig. 4 (b) and (c), respectively. Time-resolved technique allows fast data collection, and is suitable for studying phase transformation during battery operation of battery materials. In this work, the collecting time of each scan was 1 second. However, to obtain a better quality data, we report XANES spectrum from the average of 10 sequential scans. FeO

and Fe_2O_3 are used as the references for the *K*-edge of Fe when the oxidation state is +2 and +3, respectively.

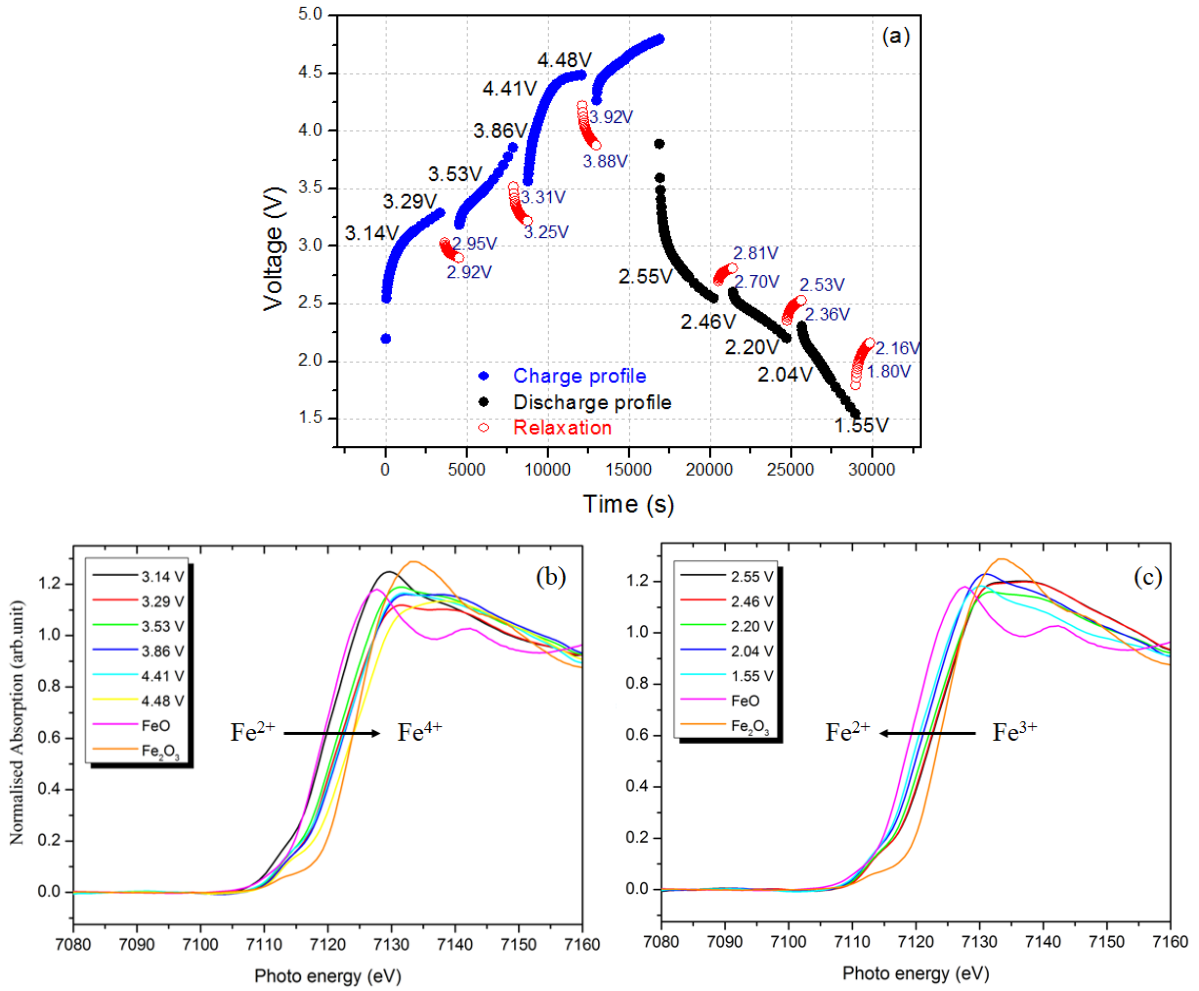

Figure 4. (a) Charge and discharge profiles of the LFS/C cathode showing the voltages at which *in-situ* time resolved XAS measurements were conducted. The corresponding *in-situ* XANES spectra at the Fe *K*-edge during charge (b) and discharge (c) are shown.

During the charge process, the XANES spectrum obtained when the electrode is charged to 3.14 V has a similar profile as of FeO indicating that the majority of Fe ion has the oxidation state of +2. The spectrum shows a slight peak shift to higher energy resulting from the partial oxidation of the Fe ion to +3 upon Li+ extraction. When we continue charging the electrode to 3.29 V, a significant shift of the XAS profile toward higher energy is observed. This means that the oxidation state of Fe ion continues to increase from 2+ to 3+ upon further extraction of Li+. When we continue charging to higher voltages at 3.53, 3.86 and 4.41 V, the XAS spectra have the *K*-edge of Fe located between the profiles of FeO and Fe_2O_3 indicating that the oxidation state of Fe is still between +2 and +3. However, no obvious shift in the *K*-edge of Fe is observed among these voltages. At these voltages, the capacities are differ by about 30 $mAh.g^{-1}$ or the different in electron transfer for $Fe^{2+}$of 0.19 e- per formula. This

means that about 19% of Fe^{2+} has transformed to Fe^{3+}, which is almost 60% difference of the amount of Fe^{3+} in the material at 4.41V compared to at 3.53 V. This should have resulted in a dramatic shift of the *K*-edge. The observed results indicate that the shift of the *K*-edge of Fe observed when voltages ranged from 3.14 to 4.41 V of LFS under the $P2_1$ space group has no linear relationship with increasing charge capacity or valence change of the Fe ions. This non-linear relationship has also been reported for LFS under the $Pmn2_1$ crystal structure [18]. Upon charging to a higher voltage at 4.48V, the XANES spectrum shifts to higher energy than that of Fe_2O_3. This suggests that the Fe ion with a high valence of +4 is formed. Note that the formation of Fe^{4+} in our LFS/C with $P2_1$ space group occurs at much higher voltages compared to the LFS with $Pmn2_1$ crystal structure observed in [18] which shows the presence of Fe^{4+} above 4.1V. The origin of this difference is still unclear but should be related to different ions arrangement in the crystal structure.

During the discharging process, the XANES spectra were obtained when the electrode were discharged to 2.55, 2.46, 2.20, 2.04, and 1.55 V as shown in Fig. 4 (c). In general, the results show the opposite trend of the shift of the *K*-edge compared to the results during the charging process, i.e. all the spectra shift to lower energy upon discharging as the Li ions are inserted back into the structure. This indicates that the valence of Fe is reduced systematically to +2 according to the degree of Li^+ intercalation in the structure. Note that the *K*-edge shift also shows no linear relationship with the discharge capacity. For example, when the electrode was discharged from 2.55 V to 2.20 V there is no obvious shift of the *K*-edge. However, the shift is very apparent when the electrode was discharged from 2.20 V to 2.04 V and a minimal shift when the electrode was discharged to 1.55 V.

3.4. Structure transformation during relaxation

In addition to *in-situ* time resolved XANES spectra during battery operation, the *K*-edge of Fe spectra of the LFS/C cathode were also collected during relaxation as shown in Fig. 5. To obtain these data, the electrode was charged or discharged to a specific voltage and allowed to relax. Several XANES spectra were collected during each relaxation and two spectra at each period are chosen to show the local structure change during relaxation. The spectra as shown in Fig. 5a were obtained at the voltages of 2.95 and 2.92 V after the electrode was charged to 3.29 V and allowed to relax. The results show that the *K*-edge also shifts to lower energy upon relaxation. Similar observations are also evident for the spectra obtained during relaxation after charging to 3.86 V (Fig. 5b) and 4.48 V (Fig. 5c). The Fe *K*-edge XANES spectra collected at 2.70 V and 2.81 V after the electrode was discharged to 2.55 V (Fig. 5d) obviously show the peak shift to lower energy. The Fe XANES spectra show a lesser but still obvious shift of the peak for the relaxation at 2.36 V and 2.53V after the electrode was discharged to 2.20 V as shown in Fig. 5e. A similar result is obtained for the relaxation at 1.80V and 2.16V after the electrode was discharged to 1.55 V as shown in Fig. 5f as well. To the best of our knowledge, these observations have not been reported before.

Shifting of the Fe *K*-edge during relaxation is surprising as we may expect that there should have been no electron transfer to cause the variation of the oxidation state of Fe-ion during relaxation. For other battery system such as $LiFePO_4$, *in-situ* time resolved XRD during high rate cycling shows

that lattice parameters *b* of both FP and LFP phases within the two-phase reaction region dynamically decrease upon high rate cycling.

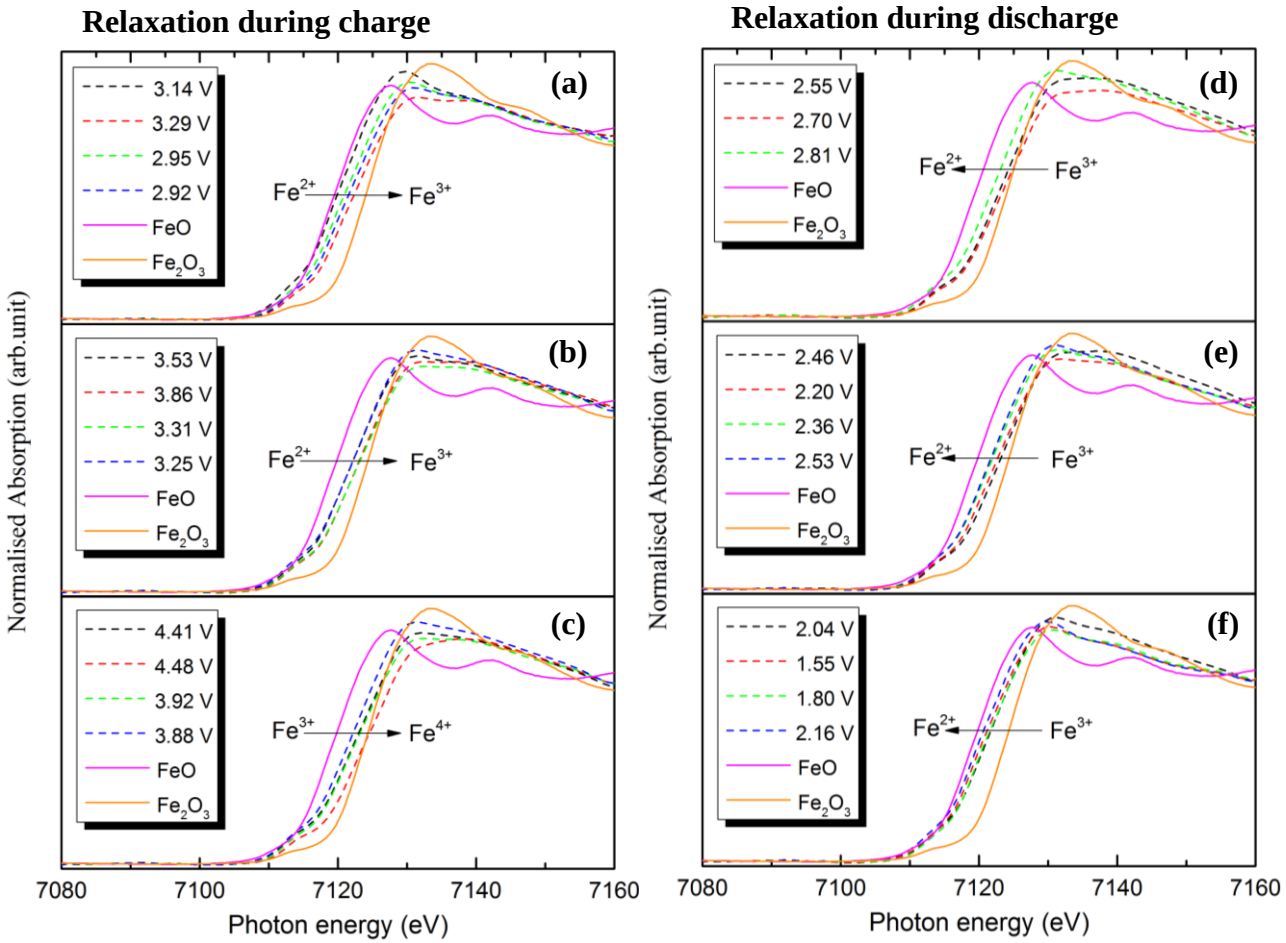

Figure 5. Normalized and calibrated Fe *K*-edge XANES spectra including the spectra obtained during relaxation at different voltages measured during the charge process (left panels) and the discharge process (right panels).

An analytical technique of XAS data, XANES difference, has been used to demonstrate that the shift of the Fe *K*-edge has been primarily correlated with the change of Fe-O bond lengths during transient phase change in olivine cathode materials [24]. For the LFS/C cathode, it may be possible that during charging and discharging, an extraction or insertion of Li ion from the structure results in an expansion or contraction of Fe-O bonds. After charging or discharging the Fe-O bond-length gradually changes and the structure eventually relaxes to an equilibrium state resulting in a shift of the Fe *K*-edge. This shows that the time-resolved XAS experiments can capture the transient changes in local structure of the LFS/C material, which has not been reported before.

4. CONCLUSIONS

Nanoscale high capacity LFS/C material with monoclinic crystal structure in space group

*$P2_1$*has been synthesized by sol-gel method using tri-block copolymer P123 as carbon source. Structural transformation during charging and discharging processes has been studied by *in-situ*time resolved XAS and the transformation of iron in the 3+ to 4+ state is responsible for high capacity of this material when charging above 4.43 V. *In-situ* time-resolved XAS experiment involves fast data collection of a second which permits us to be able to monitor fast structural and local transformation that may have been missed previously by other methods. During relaxation, the XANES spectra show a shift of the Fe *K*-edge energy (E_0) which indicates a possible variation of oxidation states or rearrangement of the ions in the structure.

ACKNOWLEDGEMENT
This work has partially been supported by the Nanotechnology Center (NANOTEC), NSTDA, Ministry of Science and Technology, Thailand, through its program of Center of Excellence Network. O.K. acknowledges support by Synchrotron Light Research Institute Scholarship GS-53-D03. W.L. acknowledges support by the Thailand Research Fund (TRF) under the TRF Senior Research Scholar, Grant No. RTA 5680008. N.M. also acknowledges support by the TRF, Grant No. MRG 5380035.

References

1. M. Armand and J. M. Tarascon, *Nature*, 451 (2008) 652-657
2. A. Nyten, A. Abouimrane, M. Armand, T. Gustafsson, J.O. Thomas, *Electrochem. Commun.*,7(2005)156-160
3. S. Zhang, C. Deng, S. Yang, *Electrochem. Solid-State Lett.*, 12 (2009) A136-A139
4. Z.L. Gong,Y.X.Li, G.N. He, J. Li, Y.Yang, *Electrochem. Solid-State Lett.*, 11(2008)A60-A63
5. S.I. Nishimura, S.Hayase, R.Kanno, M.Yashima, N.Nakayama, A.Yamada, *J. Am. Chem. Soc.*, 130(2008)13212-13213
6. C.Sirisopanapon, B. Adrien, H. DarKo, R. Dominko, B. Bojan, A.R. Armstrong, P.G.Bruce, C.Masquelier, *Inor. Chem.*, 49 (2010) 7446-7451
7. O. Kamon-in, W.Klysubun, W.Limphirat, S.Srilomsak, N.Meethong, Physica B, 416 (2013) 69–75
8. H. Guo, K. Xiang, X. Cao, X. Li, Z. Wang, L. Li, *Transactions of Nonferrous Metals Society of China*, 19 (2009) 166-169
9. C. Deng, S. Zhang, B.L. Fu, S.Y. Yang, L. Ma, *Mater. Chem. and Phys.*, 120 (2010) 14-17
10. X. Huang, X. Li, H. Wang, Z. Pan, M. Qu, Z. Yu, *Solid State Ionics*, 181 (2010) 1451-1455
11. X. Huang, X. Li, H. Wang, Z. Pan, M. Qu, Z. Yu, *Electrochem. Acta*, 55 (2010) 7362-7366
12. Z. Yan, S. Cai, L. Miao, A. Zhou, Y. Zhao, *J. Alloys and Compounds*, 511 (2012) 101-106
13. H. Zhou, M.A. Einarsrud, V.B. Fride, *Solid State Ionics*,225 (2012) 585-589
14. D. Lv, W. Wen, H. Xingkang, B. Jingyu, M. Jinxiao,W. Shunqing, Y.Yong, *J. Mater. Chem.*, 21(2011) 9506-9512
15. D. Rangappa, K.D. Murakannahally, T. Tomai, A. Unemato, T. Honma, *Nano Lett.*, 12 (2012) 1146-1151
16. A. Deb, U. Bergman, S.P. Cramer, E.J. Cairns, *Electrochim. Acta*, 50 (2005) 5200-5207
17. R.Dominko,I. Arcon, A. Kodre, D. Hanzel, M. Gaberscek, *J. Power Sources*, 189(2009)51-58
18. D. Lv, B. Jingyu, Z. Peng, W. Shunqing, L. Yixiao, W. Wen, J. Zheng, M. Jinxiao, Z. Zizhong, Y. Yong, Chem. *Mater.* , 25 (2013) 2014-2020
19. W. Xiaozhen, J. Xin, H. Qisheng, Z. Youxiang, *Electrochem. Acta*, 80 (2012) 50-55
20. W. Klysubun, P. Sombunchoo, N. Wongprachanukul, P. Tarawarakarn, S. Klinkhico, J. Chaiprapa, P. Songsiriritthigul, *Nuclear Instruments and Methods in Physics Research A*, 582(2007)87-89
21. Y. Poo-arporn, P. Chirawatkul, W. Saengsui, S. Chotiwan, S. Kityakarn, S. Klinkhieo, J. Hormes

and P. Songsiriritthigul, *J. Synch. Rad*., 19 (2012)937-943
22. B. Ravel and M.Newville, *J. Synchr. Rad*., 12(2005)537-541
23. Z. Yi, L. JiaXin, W. Ning, W. Chuxin, D. Yunhai, G. Lunhui, *J. Mater. Chem*., 22 (2012) 18797-18800
24. Y. Orikasa, T. Maeda, Y. Koyama, H. Murayama, K. Fukuda, H. Tanida, H. Arai, E. Matsubara, Y. Uchimoto, Z. Ogumi, *Chem. Mater.*, 25 (2013) 1032-1039